

Development of a 780 nm external cavity diode laser for rubidium spectroscopy

A thesis submitted in partial fulfillment of the requirement
for the degree of Bachelor of Science with Honors in
Physics from the College of William and Mary in Virginia,

by

Catherine E. Sturner

Accepted for _____

Honors

(Honors or no-Honors)

Seth Aubin

Advisor: Prof. Seth Aubin

Keith Griffioen

Prof. Keith Griffioen

Jonathan Frey

Prof. Jonathan Frey

Williamsburg, Virginia

May 2, 2023

Contents

Acknowledgements	i
List of Figures	ii
List of Tables	iv
Abstract	i
1 Introduction	1
1.1 Long Term Scientific Motivation	1
1.2 Short Term Scientific Objective	3
1.3 Structure of Thesis	5
2 Theory	6
2.1 External Cavity Diode Laser (ECDL)	6
2.2 Linewidth	8
2.3 Laser Frequency Control	10
2.4 Free Spectral Range	12
2.5 Rubidium Resonance	13
3 Construction and Set-Up	15
3.1 Insulated Housing	15
3.2 Optics	19
4 Data Acquisition	24

4.1	Initial Scanning	24
4.2	Feed-forward Scanning	29
4.3	Measuring Linewidth	34
5	Conclusion	40
5.1	Summary of Results	40
5.2	Outlook	41

Acknowledgements

I would like to thank Dr. Seth Aubin for being my first and only research advisor at William Mary these past 4 years for his continuous help and guidance, as well as the rest of the Aubin lab. I would also like to thank Dr. Keith Griffioen for his feedback and help throughout the process of this thesis. Finally, I would like to thank my friends and family for their support throughout college and this thesis. Without the phone calls, dinners, and commiseration of my friends also doing an honors thesis this thesis would not have been possible.

List of Figures

1.1	Hyperfine splitting of rubidium $5S$ and $5P$ states	3
1.2	Energy level diagram of rubidium	4
2.1	ECDL diagram	7
2.2	ECDL with the TEC and Piezo	8
2.3	Graph of the Temperature of the ECDL stabilizing	11
3.1	Actual ECDL Configuration	16
3.2	ECDL with part of old housing and stabilization	17
3.3	Picture of the temperature drift of the laser without insulation	18
3.4	Picture of the temperature drift of the laser with insulation	18
3.5	Completed ECDL housing	19
3.6	Controllers for the ECDL	19
3.7	ECDL Power vs. Current	21
3.8	Optical set-up	22
4.1	PID Settings	26
4.2	Picture of rubidium fluorescence	27
4.3	Resonance absorption curve	29
4.4	Controllers for the ECDL with the function generator	30
4.5	Graph of Current (mA) vs. Piezo Voltage (V) where mode-hops occur	32
4.6	Resonance emission curve	33

4.7	Picture of the DBR laser	35
4.8	Diagram of set-up to measure linewidth	36
4.9	Worse linewidth measurement from the ECDL	37
4.10	Better linewidth measurement from the ECDL	38
4.11	Linewidth measurement using a different laser	39

List of Tables

4.1	Effect of piezo voltage, current, and temperature on laser frequency .	24
-----	--	----

Abstract

This thesis describes the work done to improve an external cavity diode laser. These improvements consisted of constructing an insulated housing to stabilize the temperature of the laser, tuning the proportional-integral-derivative feedback of the temperature controller, achieving resonance frequencies of rubidium, and implementing and optimizing feed-forward scanning of the frequency of the laser. The laser was then successfully used to measure the linewidth of another laser in the laboratory to better understand how that laser could be best used. The knowledge gained in this thesis can also be used to change the frequency of the laser to achieve other resonances and so expand the usefulness of the laser.

Chapter 1

Introduction

1.1 Long Term Scientific Motivation

This thesis focuses on the development of a pre-existing external cavity diode laser for use in various rubidium spectroscopy experiments. The laser currently operates at 780 nm which would allow the laser to be used as a replacement or back-up laser for the current repumper laser in Professor Aubin's Ultra-cold AMO laboratory to excite the rubidium from the $5S_{1/2}$ state to the $5P_{3/2}$ state, as shown in figure 1.1. It would be useful as a replacement due to its relatively small linewidth compared to non-external cavity diode lasers, as discussed later in this thesis. Thus, there would potentially be more control in the experiment with this laser. Alternatively, it could also be used for the construction of a second laser cooling apparatus for Rydberg atom physics, by exciting atoms to a high energy level. In our laboratory specifically, lasers are used for the excitation of rubidium or potassium atoms, two alkali metals.

One of the benefits of an external cavity diode laser is that it can be tuned to a wide range of frequencies. Therefore, the main long-term goal for this laser would be to tune it to 776 nm. The laser could then be used for the Rydberg excitation of rubidium via the 5D states. In order to reach the 5D states of rubidium, one needs to use two separate lasers at two different wavelengths to excite rubidium atoms from

the $5S_{1/2}$ state. A 780 nm laser can excite rubidium from the $5S_{1/2}$ state to the $5P_{3/2}$ state, as shown in figure 1.2 in red and stated previously. From the $5P_{3/2}$ state, a 776 nm laser can be used to excite the atom up to the $5D_{5/2}$ state, as shown in blue in figure 1.2. The excitation spectra of the 5D states could be measured and the hyperfine levels identified for later use, when a Rydberg excitation laser at 1258 nm becomes available. The detection of population in the 5D states could be done by observing the emission of fluorescent photons as the rubidium atoms decay from the $5P_{1/2}$ and $6P$ states to the $5S_{1/2}$ ground state. The atoms decay through the $5P_{1/2}$ state emits photons with a wavelength of 795 nm while the atoms de-excited from the $6P$ states emit photons with a wavelength of 420 nm, as shown in figure 1.2 in purple and black, respectively. Since these wavelengths are different from the 780 nm and 776 nm excitation lasers, narrowband filters could be used to observe only the 795 nm or 420 nm fluorescence for background-free detection.

The main scientific objective for reaching the $5D_{5/2}$ state is that the atom is then only one excitation away from reaching the Stark manifold of a Rydberg level [5]. For a given principal quantum number n (e.g. $n = 50$), the Stark Manifold consists of all the high orbital angular momentum states ($l \leq 30$), at which point the energies of all these states become quasi-degenerate, as shown in the yellow box in figure 1.2. Thus, when an atom is excited to an energy level in the Stark manifold, it can easily jump to the other energy levels in the Stark manifold with little gain or lose of energy.

From an electric field sensing perspective, atoms in the Stark manifold are beneficial. This is because atoms in the Stark manifold experience a linear as opposed to quadratic Stark effect, which is the splitting of energy levels in the presence of a strong electric field [5]. Therefore, atoms in the Stark manifold are more sensitive to very small electric fields, such as from a charged particle beam, than atoms at other energy levels. Notably, the Stark manifold also has enhanced magnetic field

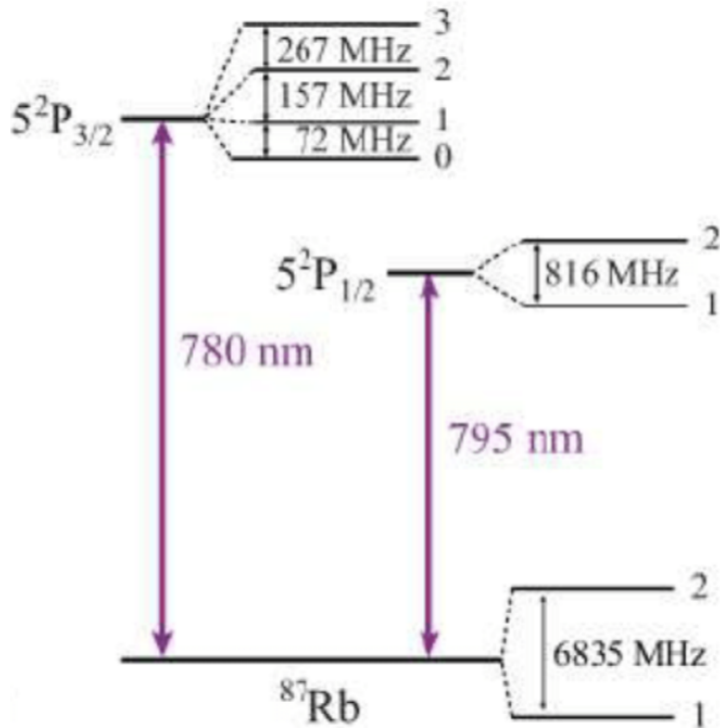


Figure 1.1: Energy level diagram of the 5S and 5P hyperfine levels of rubidium-87 at 780 nm (used for laser cooling) and 795 nm (taken from [4])

sensitivity due to its large orbital angular momentum [5].

Rubidium can be excited from the 5D states to the Rydberg levels, and thus the Stark manifold, with a 1258 nm laser, as shown in figure 1.2 in green. The 1258 nm laser could also be built as an external cavity diode laser similar to the 776/780 nm laser, allowing it the same advantages of a relatively small linewidth and tuneability of the other lasers. This 1258 nm laser would have the capabilities needed for the Quantum Enhanced Tracker collaboration, a joint Jefferson Lab and WM effort, which seeks to image charged particle beams and tracks.

1.2 Short Term Scientific Objective

The main scientific objectives of this thesis research project were to get the laser running again, stabilize it and broaden the scan range of the laser. The goal

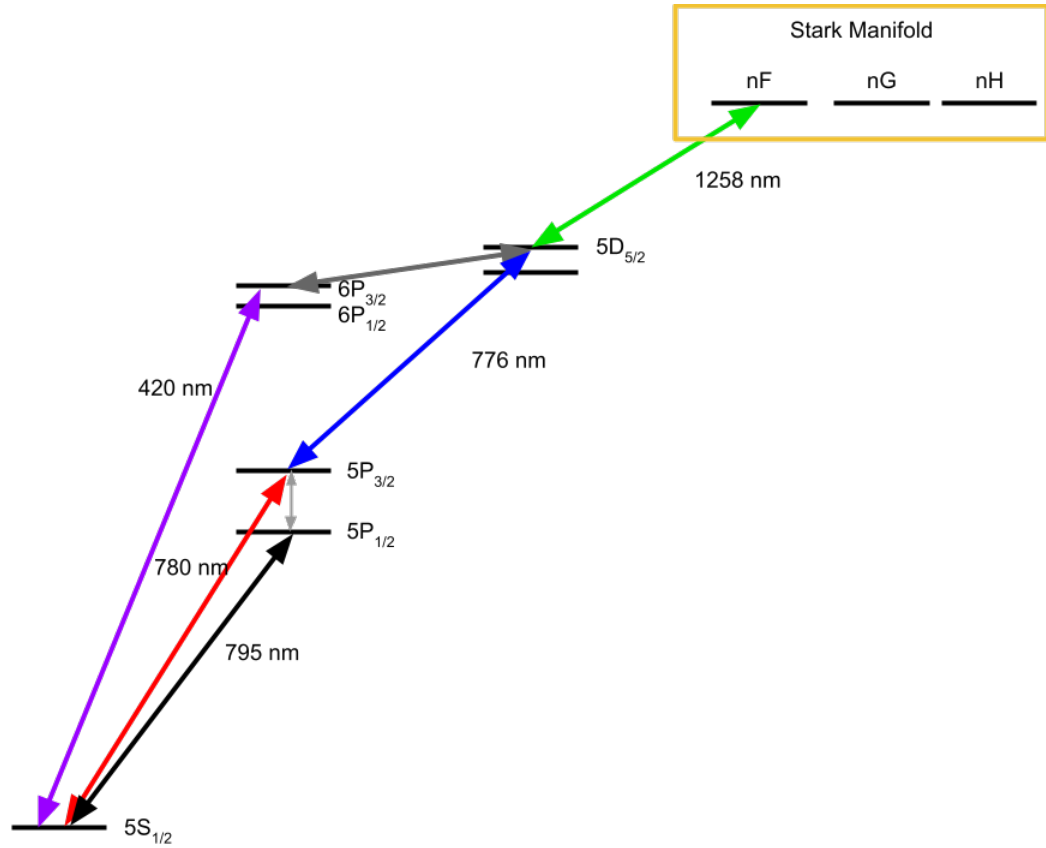


Figure 1.2: Energy level diagram showing how the lasers at different wavelengths can excite rubidium-87 atoms to different states, adapted from [3]. The atom will also emit the photons at these particular wavelengths as it decreases in energy.

for the scan range of the laser was to reach 10 GHz when the laser was tuned to 780 nm. Stabilizing the laser and increasing the scan range of the laser would allow the laser to be used under a wider set of conditions, such as various magnetic and electric fields which shift the energy levels of rubidium. In addition, with a 10 GHz scan range, the laser would be able to excite the rubidium from all the $5S_{1/2}$ states to all the $5P_{3/2}$ states, including all the different energy levels due to hyperfine splitting, Zeeman splitting, and from the Stark effect.

During the course of this thesis, the scan range of the laser was successfully increased compared to the original scan range, although the scan range did not reach 10 GHz. Nevertheless, the absorption/ emission curves due to absorption and re-

emission of photons in a rubidium vapor cell were seen. In addition, the linewidth of a separate laser was measured via its beatnote with the ECDL light, showing the ability of the external cavity diode laser to be tuned to resonance and its stability through staying on resonance long enough to measure the linewidth. Thus, these short-term scientific objectives of this thesis were broadly met.

It was hoped at the start of this thesis that the tuning and broadening of the scan range be completed within the course of a single semester and thus the laser would be able to be changed to operating at 776 nm. From there, it could have been used to excite rubidium to the 5D states as stated previously. However, the process of learning how the external cavity diode laser worked, tuning it, and establishing a larger scan range took more time than expected. Thus, this objective was not achieved and has therefore become a future goal for this project.

1.3 Structure of Thesis

This thesis is structured in the following manner. Chapter 2 provides the theory involved in the building and operating of an external diode cavity laser, including explaining what an external cavity diode laser is. It also provides more information about the energy levels of rubidium and its resonances. Chapter 3 describes the construction of an insulated housing for the laser, as well as turning on the laser and assembling an optical set-up to utilize the laser. Chapter 4 describes the process of obtaining and re-obtaining various resonances, increasing the scan range of the laser, and then using the laser to measure a separate laser's linewidth. Chapter 5 then summarizes the results of this thesis and explains future work that could be done.

Chapter 2

Theory

2.1 External Cavity Diode Laser (ECDL)

An external cavity diode laser (ECDL) has many benefits, including its relatively narrow linewidth compared to a regular diode laser, coarse wavelength tuning by small rotations of the grating, and large mode-hop free frequency tuning. A mode-hop is when the laser jumps to a different operating mode, causing the frequency to jump erratically, which is unwanted.

The ECDL utilized and further developed in this thesis was previously constructed using the Littrow configuration, shown in figure 2.1. It consists of the laser diode, a collimation lens and a diffraction grating. When the laser diode is connected to a current source of a high enough power it emits light. The light emitted from the laser diode passes through a collimation lens to a diffraction grating. The first order of the diffracted light from the grating is reflected back towards the collimation lens and laser diode, while the rest is directed away from the laser diode to be used in the experiment. Light reflected back towards the laser diode creates the external cavity, which results in the relatively narrow linewidth that is one of the largest benefits of an ECDL. The Littrow configuration was chosen for its relative ease of construction compared to the other main ECDL configuration, the Littman-Metcalf

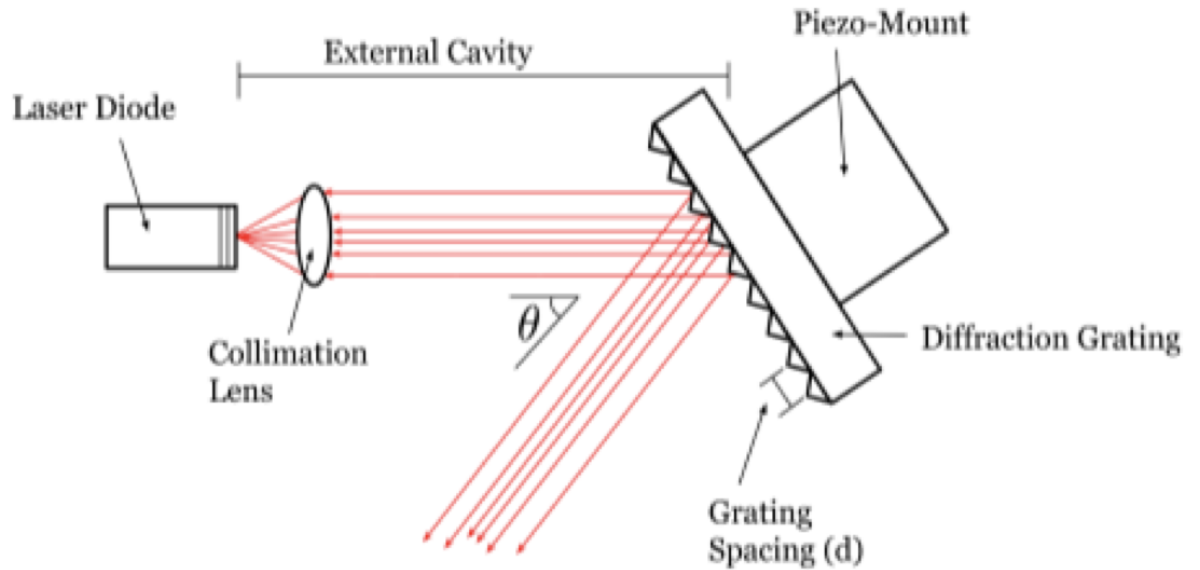


Figure 2.1: Diagram of the ECDL, showing the main components of the laser system (taken from [1]). The light from the laser diode is directed at the diffraction grating, causing some of the light to be reflected back to the laser, narrowing its linewidth.

configuration, and due problem to the of large power losses with the Littman-Metcalf configuration [10].

In addition to the basic Littrow configuration of the ECDL, the particular laser in this experiment also includes other features that give more control over the output light. A thermoelectric cooler (TEC) was placed underneath the laser diode, as shown in figure 2.2, to control the temperature of the laser. Also, the diffraction grating was attached to a piezo, shown in figure 2.2, which adjusts the diffraction angle based on the amount of voltage sent to the piezo. This allows for more accurate control of the diffraction angle.

The frequency of the light emitted from the ECDL can be changed through various factors. This includes the grating spacing, d , as shown in figure 2.1. The frequency of the laser can also be changed through changes in the input current, the temperature

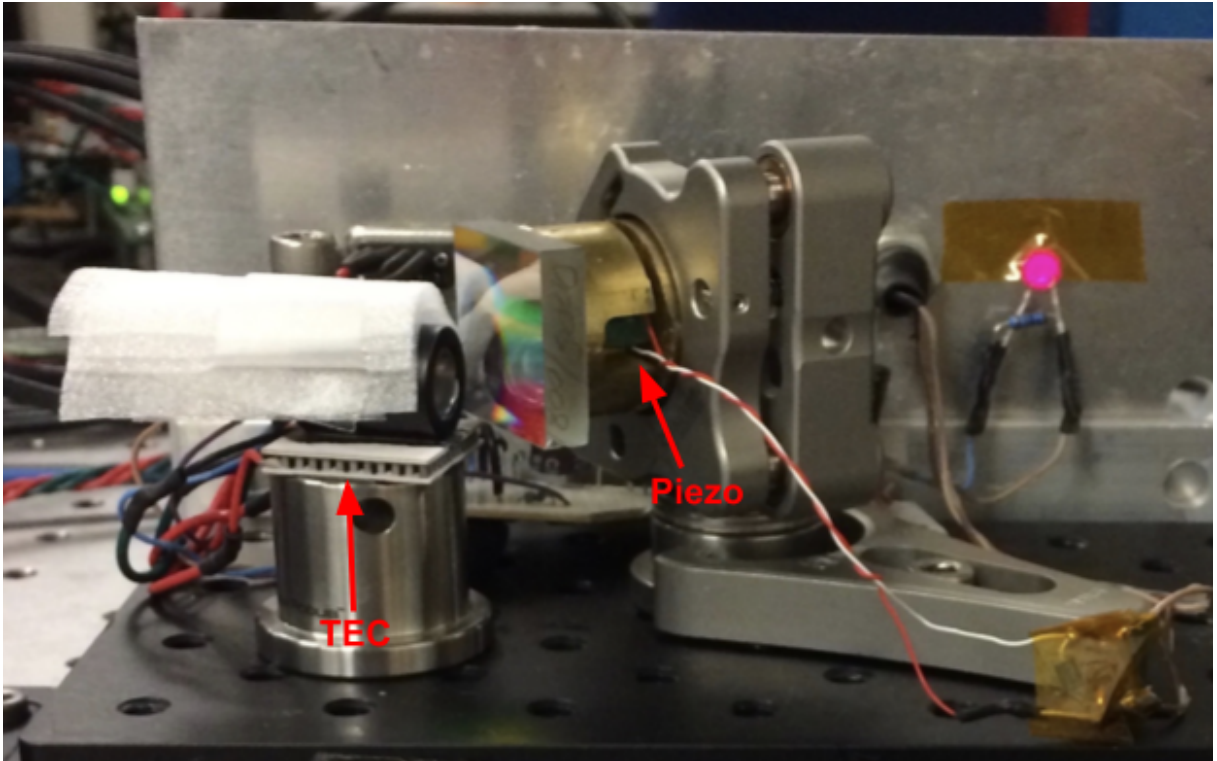


Figure 2.2: This picture shows the ECDL with the thermoelectric cooler (TEC) shown underneath the laser diode as labelled, and the piezo attached to the diffraction grating and piezo mount as labelled. Adapted from [1].

of the diode, and the diffraction angle (θ), and thus the piezo voltage. This is why the added control from the TEC and piezo is important.

2.2 Linewidth

The linewidth of a laser is the narrow range of wavelengths the laser emits at one time, as they do not emit light of a single wavelength but instead a range that is usually symmetric about the maximum wavelength. While it is not currently feasible to have a laser with no linewidth, the narrowest linewidth possible is usually preferred. This is because the narrower the linewidth, the more control and precision one has in an experiment [9]. Therefore, the narrow linewidth of the ECDL is one of its main advantages.

It is not usually possible to measure the linewidth of a laser directly using a

spectrum analyzer as most do not go up to high enough frequencies. One method to measure the linewidth of a laser is to couple it with another laser with a known very narrow linewidth. Then, the linewidth of the resultant beat note provides a measure of the linewidth of the laser under investigation. The measure of width used is the full width at half the maximum (FWHM) of the beat note.

The beatnote appears due to the electromagnetic wave nature of light. Therefore, the light from the lasers can be described using the the following equation for the electric field of a laser,

$$\bar{E} = e^{i\omega t}, \quad (2.1)$$

where \bar{E} is the electric field, ω is the frequency, and t is time [11]. In equation 2.1, the amplitude and the space components are omitted for simplicity, as they are not relevant to showing how the beatnote is used to find the linewidth of the laser under investigation.

When the electric fields from the two lasers are combined, the electric fields are added together. The combined electric field is then sent to a photodetector, which measures the power of the field at the frequencies they occur. The power is the square of the electric field, given by the equation

$$P = (e^{i\omega_1 t} + e^{i\omega_2 t})^*(e^{i\omega_1 t} + e^{i\omega_2 t}), \quad (2.2)$$

where P is the power and ω_1 is the frequency of the one laser and ω_2 is the frequency of the other laser [11]. Thus, the frequencies at which the laser has any power are $2\omega_1$, $2\omega_2$, and $-\omega_1 - \omega_2$. However, since $2\omega_1$ and $2\omega_2$ are larger than the frequencies of the input lasers, they are also unlikely to be able to be detected by a spectrum

analyzer. Thus, the frequency that will be detected is

$$\omega_{beatnote} = |\omega_1 - \omega_2|, \quad (2.3)$$

where $\omega_{beatnote}$ is the frequency at which power is measured from the combined field of two lasers, known as the beatnote. Since the laser under investigation has a large linewidth, or range of frequencies, compared to the known laser, the linewidth of the resultant beatnote will be mostly due to the unknown laser. For the ECDL used in this thesis, the linewidth was previously measured to be less than or equal to 0.5 MHz [2].

2.3 Laser Frequency Control

During the course of a typical experiment, the wavelength and frequency are controlled by adjusting the piezo voltage, the current sent to the laser diode, and the temperature of the laser diode.

Adjusting the piezo voltage changes the diffraction angle and cavity length in the ECDL, thus controlling the wavelength of the laser output. This happens because adjusting the piezo results in the piezo moving forward or back depending on whether the voltage is increased or decreased. This changes the location of the diffraction grating and thus the diffraction angle and cavity length.

The ECDL used in this experiment is in the Littrow configuration. Thus, the equation relating the diffraction angle to the wavelength is

$$n\lambda = 2d(\sin\theta), \quad (2.4)$$

where n is the order of diffraction, λ is the wavelength of the diffracted light, θ is the angle of diffraction [12].

Another way to adjust the frequency is to change the current sent to the laser diode. The current affects the refractive index in the laser diode [13]. Changing the

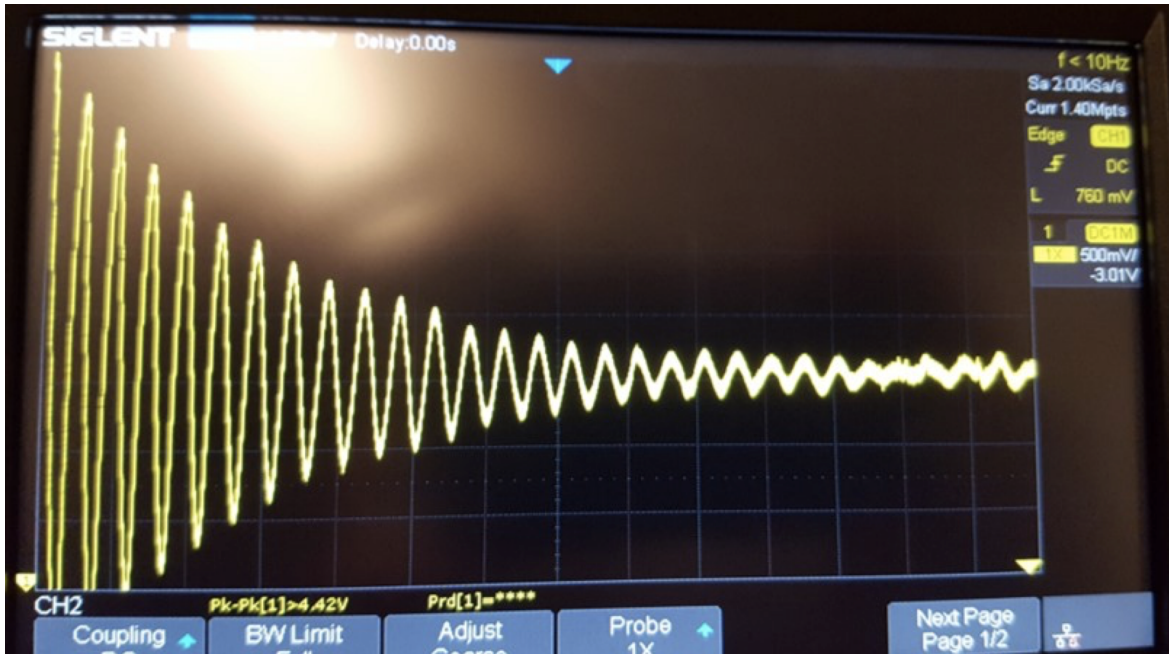


Figure 2.3: This picture shows the measurement from the temperature controller. The vertical axis is the temperature while the horizontal axis is time. From the measurement, one can see that the temperature is oscillating more when the temperature is first taken, which is due to the change in temperature, but it stabilizes as time progresses and it continues to oscillate, settling to the set temperature. Taken from [2].

refractive index then alters the frequency of the light emitted from the diode and thus the frequency of the light that is output by the ECDL.

The final factor in this thesis that will be used to adjust the frequency is the temperature. When the temperature changes, the center frequency amplified by the gain medium shifts. The temperature will be both set and stabilized using a Peltier Thermo-electric Cooler (TEC), as mentioned earlier. When the temperature controller is set to a new temperature, the TEC quickly tries to reach this new temperature. This often results in the TEC overshooting the desired temperature and then over-correcting itself. Thus, the temperature will oscillate about the desired temperature, slowly decreasing in amplitude until it finally settles at the set temperature, as seen in figure 2.3. Thus, the temperature is the most difficult factor to control and will be adjusted the least.

It is important to note that changing the current tends to also change the temper-

ature of the ECDL. This means that the current needs to be adjusted slowly in order to not destabilize the frequency by both the current and the temperature rapidly changing.

2.4 Free Spectral Range

The free spectral range (FSR) of a laser is the approximate frequency span in which it is expected to be able to tune a laser without a mode hop. It does not take into account other effects that may destabilize the laser, such as changes in temperature or vibrations.

The FSR for the laser used in this experiment can be calculated using the equation,

$$FSR = \frac{c}{2 \cdot L} = \frac{c}{2 \cdot 12 \cdot 10^{-3}m} = 12.5GHz, \quad (2.5)$$

where c is the speed of light and L is the distance from the back of the diode cavity to the grating. For this ECDL, $L = 1.2$ cm approximately, which takes into account the length of the diode itself and distance to the grating, as well as the change in material.

Thus the expected maximum tuning span for the ECDL in this experiment without mode hops is 12.5 GHz. This is only an approximation, however, due to other factors that can lead to mode hops. One way to try to achieve this scan range, however, is through feed-forward scanning [6]. Feed-forward scanning involves changing the current and piezo voltage of the ECDL in such a way that they both increase or decrease the frequency of the laser output simultaneously, increasing the scan range of the ECDL before a mode-hop [6].

2.5 Rubidium Resonance

The ECDL in this experiment is meant to be used to excite rubidium-87. In particular, it was designed to originally excite rubidium from the $5S_{1/2}$ state to the $5P_{3/2}$ state, hence why it was tuned to approximately 780 nm to achieve this transition as shown in figure 1.1. The exact wavenumber needed to excite ^{87}Rb from the $5S_{1/2}$, $F = 1$ state to the $5P_{3/2}$, $F = 2$ state is $12816.693 \text{ cm}^{-1}$, which is the reumper transition used in laser cooling. This is known as a rubidium resonance.

This rubidium resonance can be detected using a rubidium vapor cell. When the laser is passed through the vapor cell at the proper frequency stated previously, it excites the rubidium to the higher energy level. This energy is later spontaneously emitted, resulting in the emission of a photon with the frequency corresponding to the emitted energy, $E = \hbar\omega$.

The wavelength of the emitted light by the rubidium in the vapor cell is near-infrared (780 nm). This light is therefore difficult to observe with the naked eye. Thus a security camera sensitive to near-infrared light was connected to a CCTV to more easily monitor whether a rubidium resonance was achieved.

The rubidium inside of the vapor cell is moving due to its thermal energy. Therefore, the rubidium has a Maxwellian distribution of velocities. The velocity of the atoms affects the wavelength of the light needed to excite the atoms due to the Doppler Effect. Since there is a distribution of velocities and a range directions of velocity relative to the laser light, there will be a range of frequencies around the expected 780 nm that will result in a resonance.

These resonances are expected to be Gaussian peaks with a FWHM as defined by the equation

$$\Delta v_{1/2} = \sqrt{8k_B \ln 2} \frac{v_1}{c} \sqrt{\frac{T}{M}} = 2.92 \times 10^{-20} v_1 \sqrt{\frac{T}{M}} \text{ Hz}, \quad (2.6)$$

where $\Delta v_{1/2}$ is the FWHM, T is room temperature (about 300 K), M is the mass of rubidium (about $87 \times 1.67 \times 10^{-27}$ kg, and ν_1 is the rest frequency (about 3.85×10^{14} Hz [14]. Plugging these values into equation 2.6, the expected FWHM is about 500 MHz. This value is much larger than the linewidth of the laser. Therefore, it will be possible to see the shape of the resonance peaks as the laser's frequency scan over the broadened resonance.

Chapter 3

Construction and Set-Up

In previous experimentation, the instability of the temperature was studied. The ECDL initially had no housing, as shown in figure 3.1. However, in order to protect the inner workings of the ECDL, a metal housing was added for vibrational and temperature stabilization, as well as to provide a control panel, as partially seen in figure 3.2.

With this initial housing, the temperature instability was measured [2]. Periodically in the study of the temperature, sudden changes, or kicks, in the temperature occurred, as seen in figure 3.3. In order to test the source of these kicks, a temporary additional insulating box was added. The improvements from this insulation are shown in figure 3.4. Since the insulation got rid of these sudden changes in the temperature, it was decided that the kicks were due to air currents and therefore new, permanent insulation was needed to improve the ECDL.

3.1 Insulated Housing

My first task in for this project was to construct the new, permanent insulated housing for the ECDL. I based my design on previous work done by Quinton Olson [2]. I used 1 cm thick acrylic to construct the outer box, as pictured in figure 3.5. One important aspect I needed to consider was a way to connect the box to the base

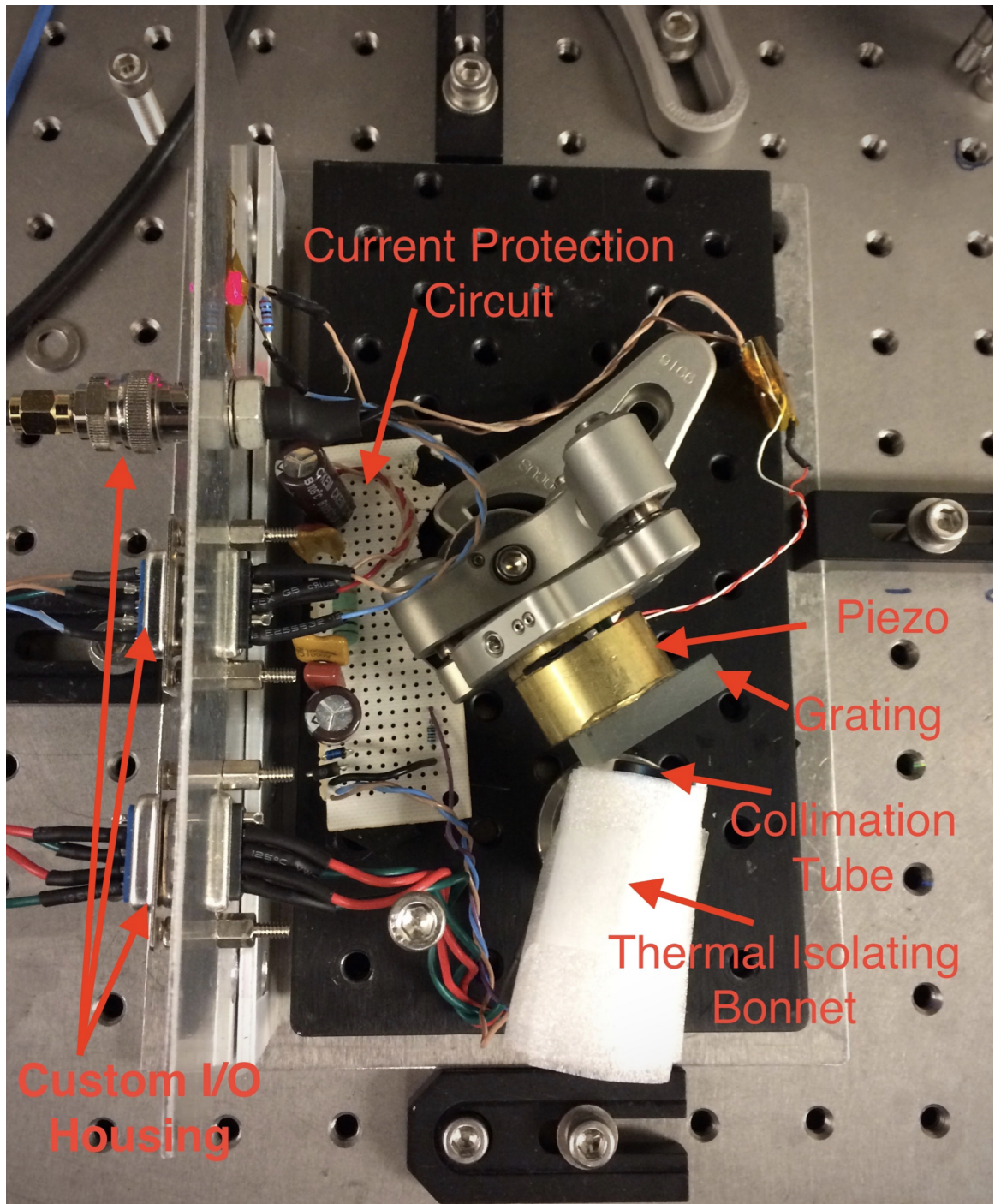


Figure 3.1: Picture of the actual ECDL used in this thesis. It consists of the diode on top of the Peltier TEC with a thermal isolating bonnet. The light then travels through a collimating tube to the grating attached to a piezo. The picture also shows the circuit connecting the piezo, laser diode, and TEC to their controllers. Taken from [1].

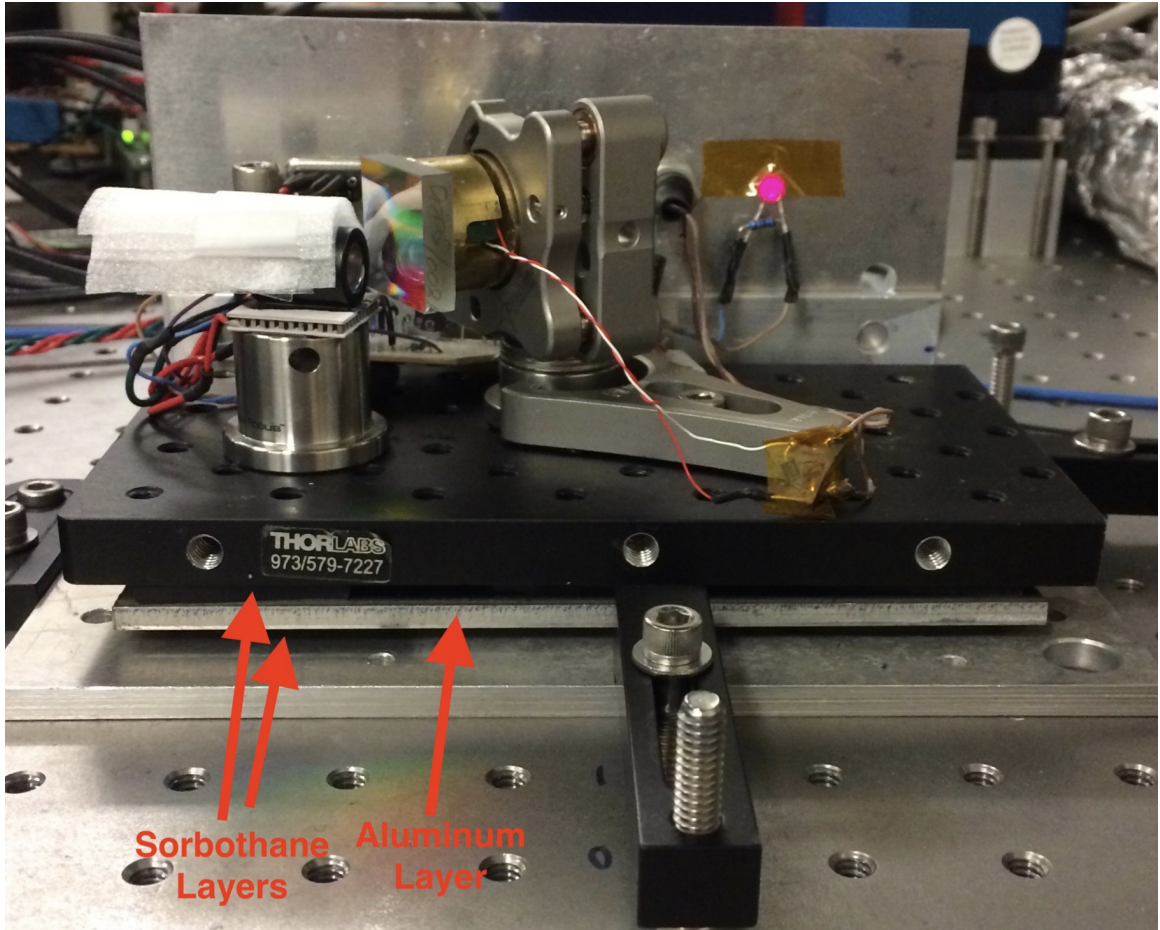


Figure 3.2: This picture shows a better view of the ECDL inside of its old housing, which includes the metal wall behind the ECDL. The rest of the metal box was removed to access the ECDL itself. The housing also consists of sorbothane and aluminum layers to isolate the ECDL from vibrations. Taken from [1].

that the ECDL sits on. This was necessary in order to guarantee the stability of the housing, as well as to ensure that the laser output would not be blocked by any shifts in the insulated housing. Thus, I installed feet at the bottom of two sides of the house with holes spaced at the same distance as the screw holes on the base of the ECDL. I was then able to attach the housing to the ECDL base with $\frac{1}{4}$ -20 screws.

Another aspect I needed to consider was the electrical ports for the current, temperature controller, and piezo voltage. In order to easily install and remove the insulated housing, I placed the ports on a separate panel from the rest of the box. The panel then connects to the box with two screws and bolts to secure it. Thus, I

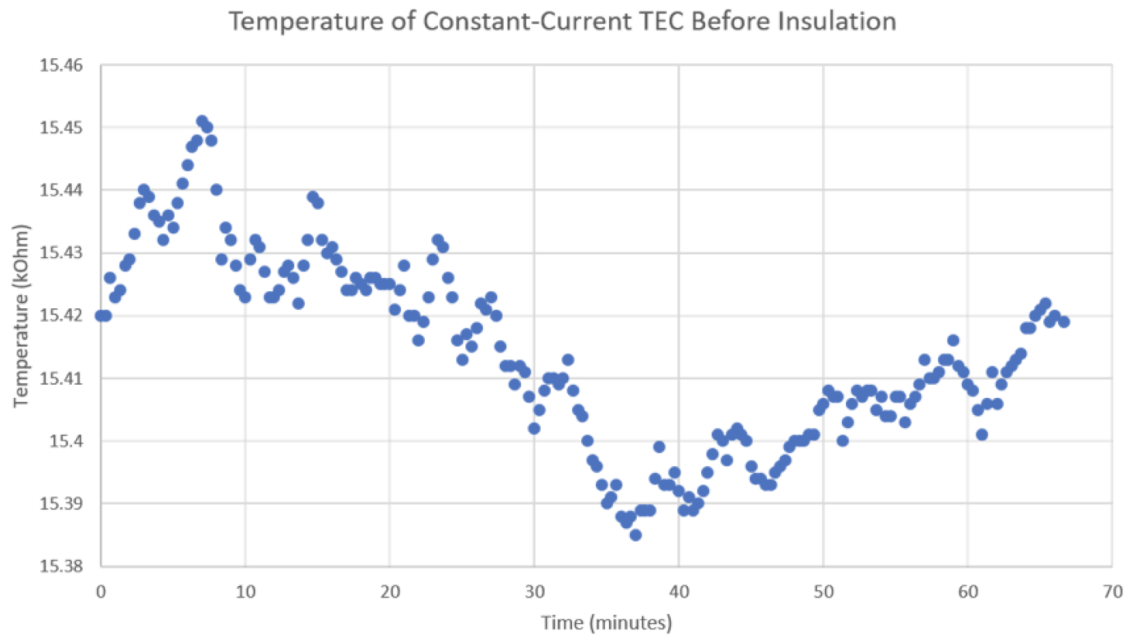


Figure 3.3: Graph of the drift of the temperature over time without insulation. It is possible to see the short term kicks in temperature. Taken from [2].

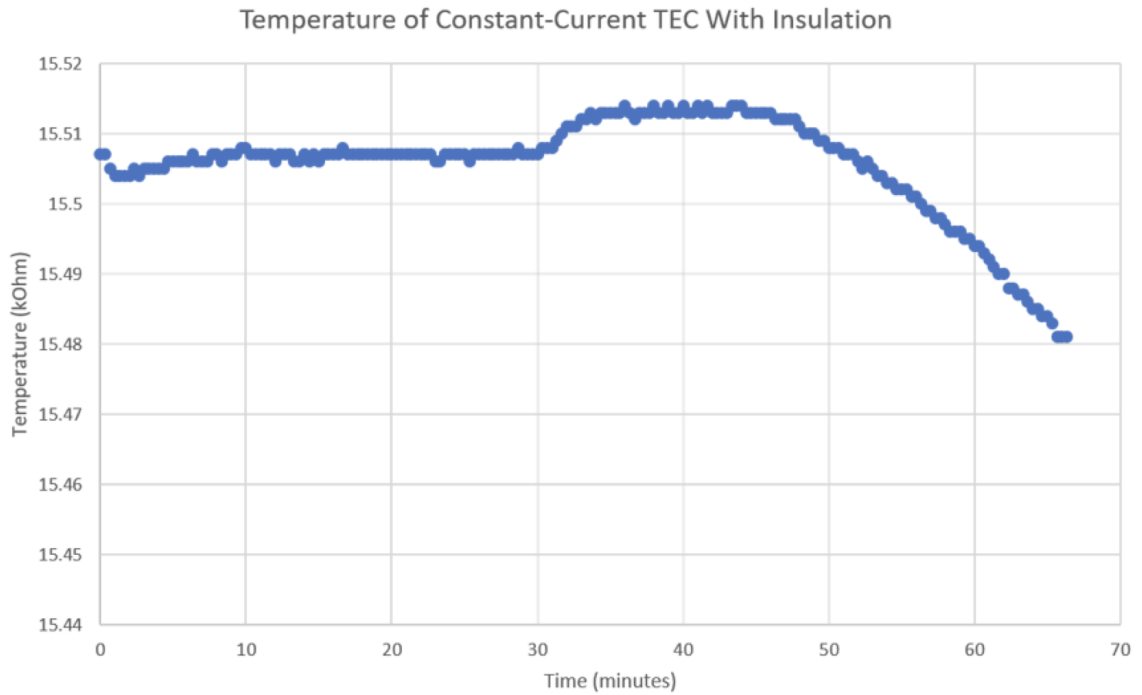


Figure 3.4: Graph of the drift of the temperature over time with insulation from air currents. Since there is no short term variation, it was decided that air currents were the primary cause of the temperature drift. Taken from [2].

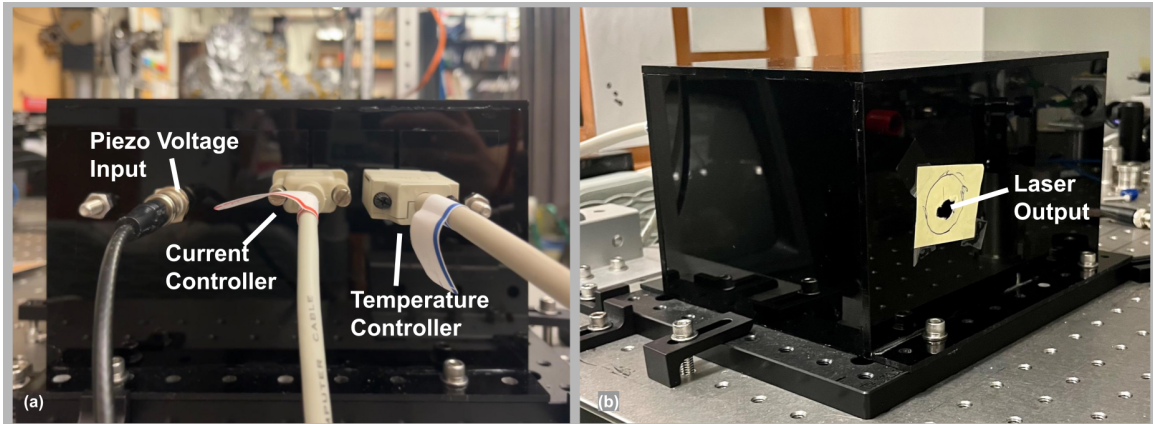


Figure 3.5: Pictures of the ECDL with completed insulated housing. (a) Picture of the control panel for the laser. The inputs are a voltage input to control the piezo, current input, and a temperature sensor and controller. The input values are changed to change the wavelength/ frequency of the laser. (b) Picture of the other side of the insulating housing where the laser light is emitted. The housing attaches to the base of the laser is attached to which is then screwed to the optics table.

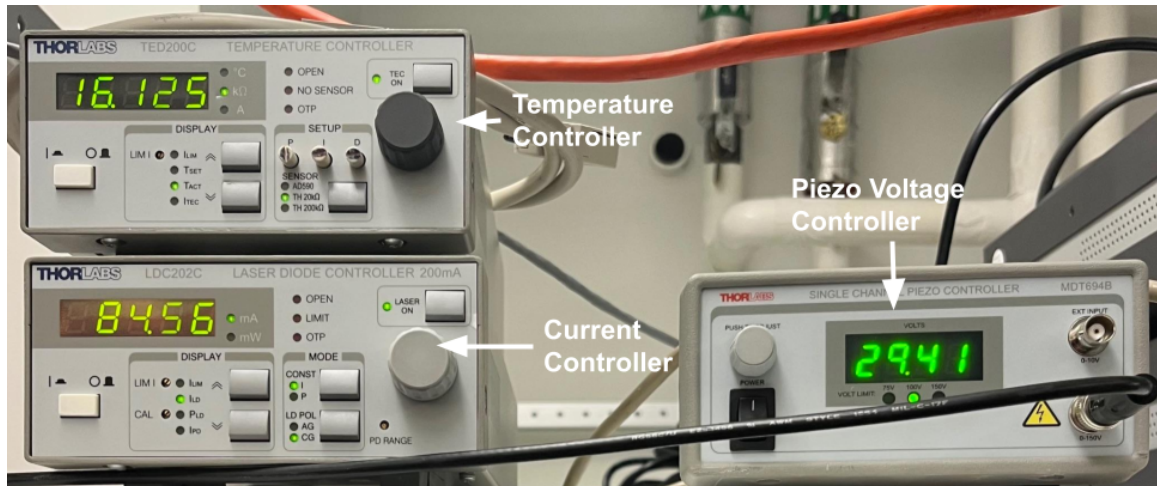


Figure 3.6: Picture of the control boxes for the ECDL, with the temperature controller and current controller on the left and the piezo voltage controller on the right.

was able to attach the temperature controller, current controller, and piezo voltage controller (see fig. 3.6) to the ECDL.

3.2 Optics

With the insulated housing complete, the next step was to turn on the laser and test it.

Lasing Threshold

The first test for the laser once the new housing was installed was to find the lasing threshold. This is the minimum current at which there is light output from the ECDL. This is important for later, when I am setting or scanning the current, so that I know at what point there will no longer be light from the ECDL.

The lasing threshold was obtained by directing the laser beam into a powermeter to measure the output power from the laser. The current was set to various currents, from 0 mA to the maximum allowed current rated for the laser diode, 100 mA. The data, shown in figure 3.7, fit the basic theory, as it was constant until the lasing threshold and then increased linearly with the current. The data in which the output power from the laser was greater than 0 mW was then fit to a linear polynomial, $P = aI + b$, where P is the power and I is the current. The lasing threshold was then found by setting the power to 0 mW in the equation of best fit and solving for the corresponding current. From this equation of best fit and the data in figure 3.7, the lasing threshold was found to be 34.6 mA. Overall, this was a good initial test to ensure the laser was working as expected. The lasing threshold at 34.6 mA also means that the range of the current is about 65 mA, which is large enough to provide adequate scanning of the current to achieve the resonance frequencies.

Optics Set-up

With the laser initially tested for proper operation, it was time to assemble the optics set-up for the experiment. The set-up is shown in figure 3.8.

The laser output light was reflected off two mirrors, and then into an optical diode. The two mirrors allow for easier alignment into the optical diode, as the first mirror primarily translates the laser beam, while the second mirror largely adjusts the angle at which the beam hits the optical diode. The optical diode was used to prevent light

Power (mW) vs. Current (mA)

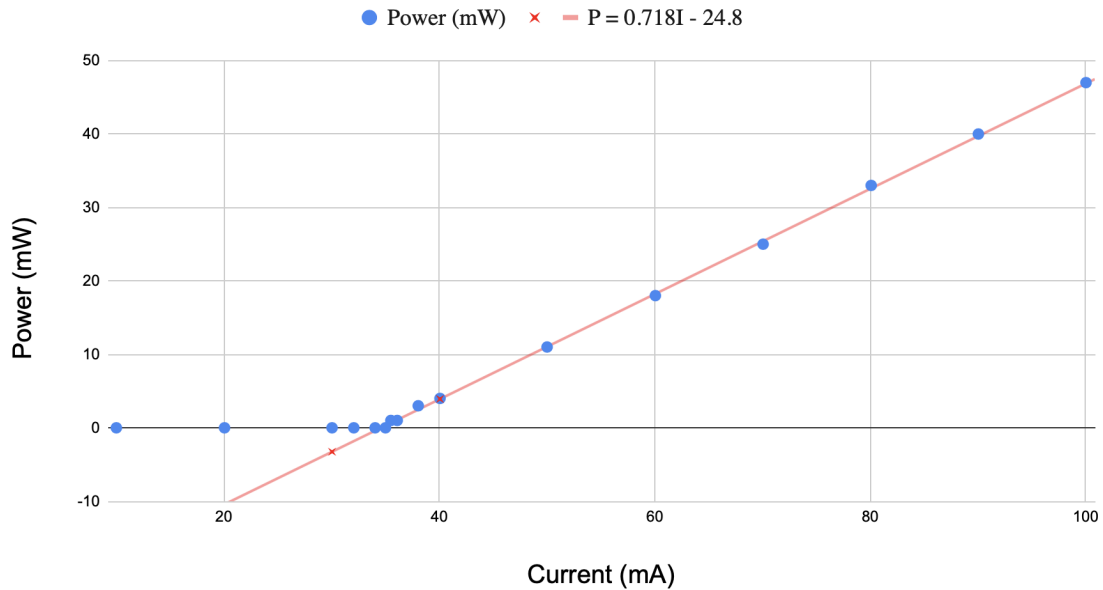


Figure 3.7: Graph of the power output from the laser versus the current provided to the laser diode. The piezo voltage was 0V, and the laser was at room temperature. The red line, $P = 0.718I - 24.8$, is the line of best fit for when the laser output power was greater than 0 mW.

from reflecting from later in the experiment back into the ECDL such a spurious reflection would create a secondary external cavity, decreasing the FSR of the ECDL and increasing the mode hops. However, some laser light is reflected back from the input of the optical diode and not transmitted. This would turn out to be a problem later in the experiment.

The light needed to pass through optical diode at the right angle in order to ensure that a significant portion of the light is able transmit it without distortion. Thus, I used a powermeter to test the laser's power before and after the optical diode. As I adjusted the two mirrors before the optical diode, the power transmitted would increase or decrease. Once I got the laser beam to hit the crystal in the optical diode, I mainly adjusted the second mirror to change the angle and exact placement of the laser beam to optimize the transmission. The final percentage of the light into the

coupling. It was aligned until there was a few mW of power output from the fiber at 70 mA of current, with the exact power depending on the current of the laser diode, as seen previously when finding the lasing threshold. This would provide enough power for the wavemeter to measure the wavenumber of the laser.

A smaller percentage of the laser beam was reflected off the glass and towards the rubidium vapor cell in order to hopefully see the rubidium resonances. A camera was placed in the set-up to view the vapor cell and send the live video to a CCTV that has the ability to see the near-infrared resonance light more clearly than with the naked eye. In addition to the camera, a photodiode was placed in the path of the laser through the vapor diode. The photodiode would measure less light when a resonance was achieved as photons would be absorbed by the rubidium and re-emitted in random directions. Thus, there were two ways to detect that the laser was on a resonance.

Chapter 4

Data Acquisition

4.1 Initial Scanning

The first step to scanning for the rubidium resonance was to figure out how changing the piezo voltage, current, and temperature affected the laser frequency. The relationship between these parameters and frequency is shown in table 4.1.

Table 4.1: Effect of piezo voltage, current, and temperature on laser frequency

Parameter	Increase Frequency	Decrease Frequency
Temperature (Thermistor Resistance)	Decrease (Increase R)	Increase (Decrease R)
Piezo Voltage	Increase	Decrease
Current	Decrease	Increase

When scanning the range of the laser, the frequency would mode-hop every 0.1 GHz, as opposed to every 12.5 GHz, i.e., the expected FSR. While it is unlikely that the experimental FSR would be the same as the theoretical FSR due to various problems of stability when practically implementing an ECDL, the orders of magnitude difference was cause for some concern.

One possible cause of the drastically decreased FSR was due to the creation of a large optical cavity outside the ECDL housing. This would then increase L in the equation 2.5, decreasing the FSR. Since the optical diode would prevent the light from the laser from being transmitted from anywhere between it and the fiber back

towards the ECDL, the cavity was likely from before the optical diode. It was found that the laser beam was reflected off the front side of the optical diode as it entered the diode. The reflected light then followed the path of the laser back into the laser box. This large cavity was eliminated by shifting the optical diode at a small angle such that the reflected light would not follow the same path as the incident light. After this change, while the FSR was still smaller than expected, the frequency was more stable.

PID Settings

During the course of trying to achieve a resonance and adjusting the set temperature of the laser, the temperature stopped settling, continuing to oscillate for hours. The temperature controller requires tuning of the proportional, integral, and derivative (PID) values in order to get optimal control [7]. Thus, I adjusted the PID settings of the temperature controller, changing each individual value in small increments and waiting a couple minutes to see how it affected the rate at which the temperature reached the set point. I continued adjusting until the resistance corresponding to the temperature of the controller settled to about $\pm 0.001 \text{ k}\Omega$ from the set temperature from $\pm 0.015 \text{ k}\Omega$ in approximately 5 minutes. This resulted in the PID values being set as shown in figure 4.1.

Achieving Resonance

With the laser light now more stable, it was time to tune the laser frequency to a resonance frequency. In order to achieve a resonance, I first tried to use values for the current, temperature, and piezo voltage that had previously resulted in a resonance by others. However, I was unable to not only get on resonance, but I was also unable to get close to the resonances at approximately 12816 cm^{-1} . Therefore, I started by adjusting the temperature as changing the temperature yielded the biggest change in

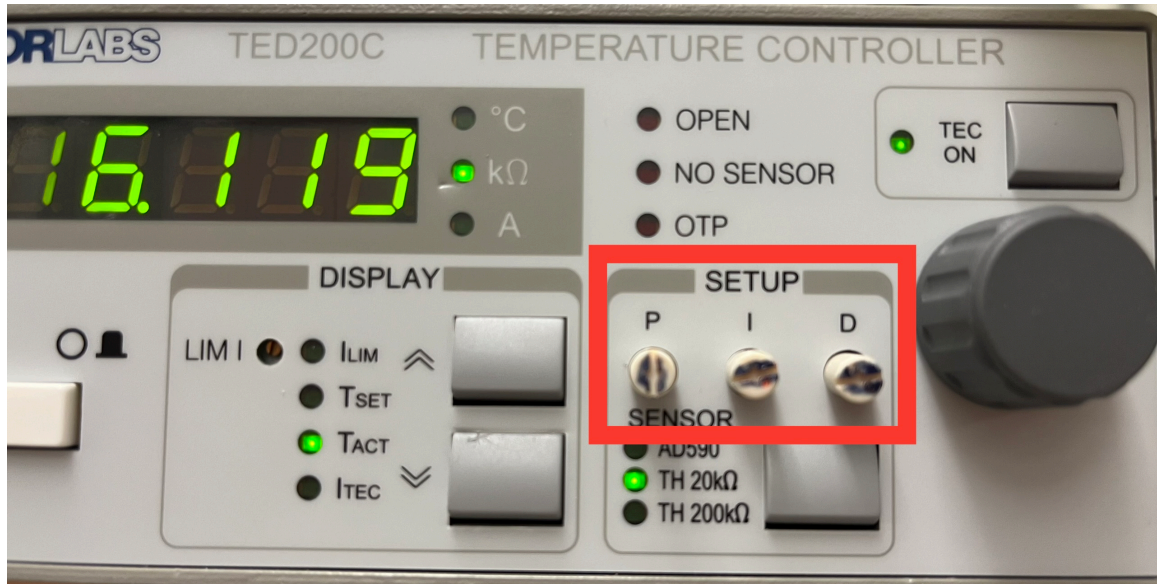


Figure 4.1: Picture of the final PID settings for the temperature controller.

frequencies. In changing the temperature, I needed to ensure that the temperature remained above the dew point of the air, as a temperature below the dew point may have resulted in water forming on by the diode, decreasing the stability of the ECDL. Once the temperature settled, I would then adjust the piezo voltage and current to try and get close to the resonances.

Finally, a resonance was achieved at a temperature of 14.7°C (resistance = $16.125\text{ k}\Omega$), current of $I = 84.56\text{ mA}$, and piezo voltage $V = 29.41\text{ V}$. The resonance achieved was at the wavenumber 12816.48 cm^{-1} and is shown in figure 4.2.

I then changed the settings to achieve more resonances, keeping the temperature resistance constant at $16.115\text{ k}\Omega$ and the piezo voltage constant at $V = 22.61\text{ V}$ and adjusting just the current. When the laser mode-hopped to other frequencies, I was able to reattain the resonance with relative ease. Returning to the resonance often requires scanning the current above and below the value that the resonance originally occurred at, at least once if not multiple times, due to hysteresis of the laser frequency [8].

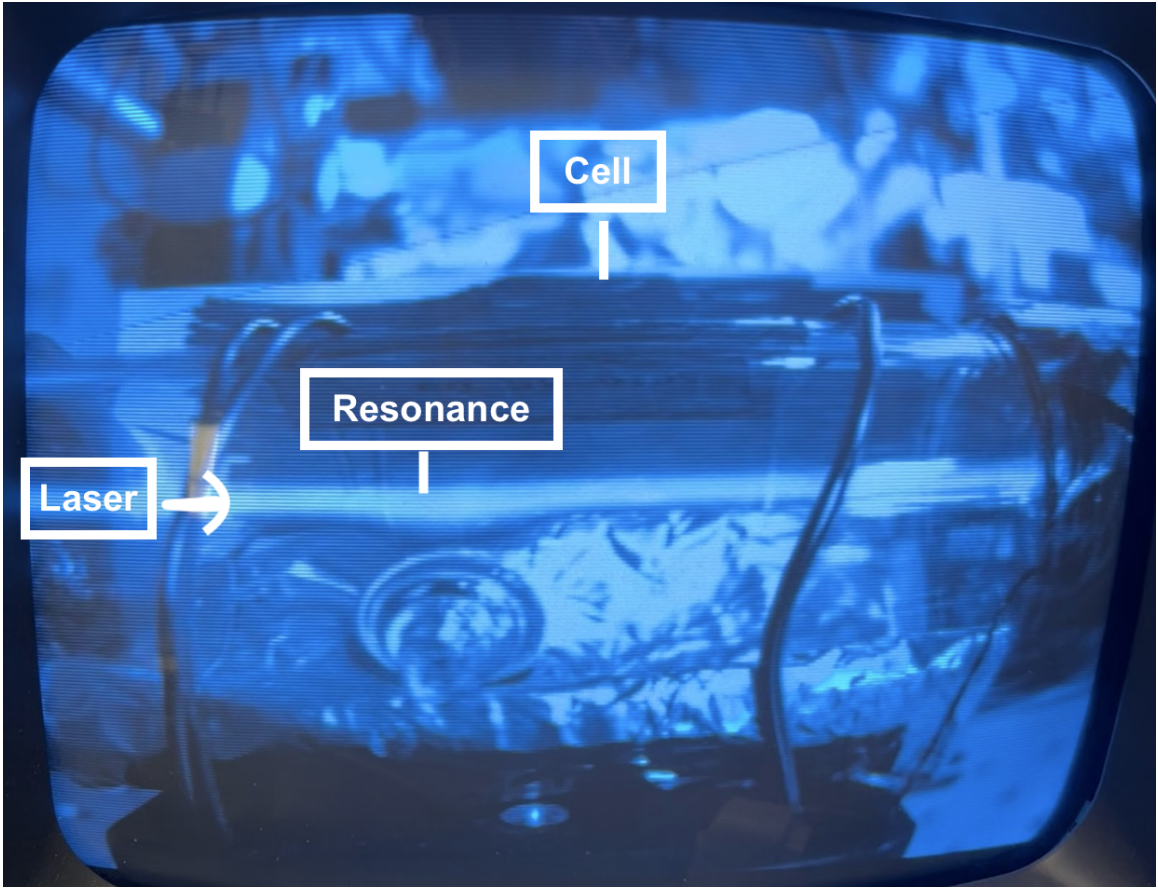


Figure 4.2: Picture of the fluorescence from the rubidium vapor cell due to the resonance being achieved.

Throughout my work trying to achieve different resonances, I started to see the pattern in the mode-hopping of the laser's frequency. First of all, the laser seemed to mode-hop to certain frequencies which would shift as the different variables were increased or decreased. For example, when the TEC was set to a resistance of 16.115 k Ω and the piezo voltage was at $V = 22.61$ V, the wavenumber of the laser would tend towards the approximate values of 12820 cm^{-1} , 12816 cm^{-1} , and 12806 cm^{-1} as the current was increased. The laser would mode-hop to these values in this order several times as the current increased from 40 mA to 90 mA. However, since the frequency and thus the wavenumber of the laser decreases as the current increases, the exact value the laser would mode-hop to would decrease as the current increased.

For example, when increasing the current from 70 mA, the laser might start at 12820 cm^{-1} , then go to 12817 cm^{-1} , and then go to 12807 cm^{-1} . As the current continued to increase, though, the wavenumbers may then be 12819.8 cm^{-1} to 12816.8 cm^{-1} to 12806.6 cm^{-1} . Thus, I was able to tell when I was getting close to achieving the resonance. These values would also change if one decreased the current instead of increasing the current due to the hysteresis of the wavenumber.

Overall, I achieved resonances at approximately 12816.69 cm^{-1} , 12816.60 cm^{-1} , 12816.52 cm^{-1} , and 12816.48 cm^{-1} . When the photodiode was configured to detect emission, the brightest resonance was at 12816.52 cm^{-1} , which had a detected emission of about 50 mV from the photodiode, whereas the next brightest emissions detected were about 30 mV from the 12816.48 cm^{-1} and 12816.60 cm^{-1} resonances.

With this milestone achieved, I moved on to scanning the frequency at a resonance by manually adjusting the current and piezo voltage. I was able to see the absorption curve of the resonance with the photodiode. As shown in figure 4.3, the measurement from the photodiode started large as most of the light was able to travel through the rubidium vapor cell without being absorbed. It then decreased due to the light being absorbed by the rubidium and then being re-emitted in other directions and increased again as the frequency again went off resonance.

With manual scanning of just the current or just the piezo I was able to achieve a maximum scan range of approximately 0.01 cm^{-1} , or 0.3 GHz, which is much less than the goal of a 10 GHz scanning range. Through manually adjusting both the piezo and the current simultaneously in a feed-forward manner, I was able to get a scan range of approximately 0.8 GHz. This showed the importance of the feed-forward aspect of scanning to get a larger scan range.

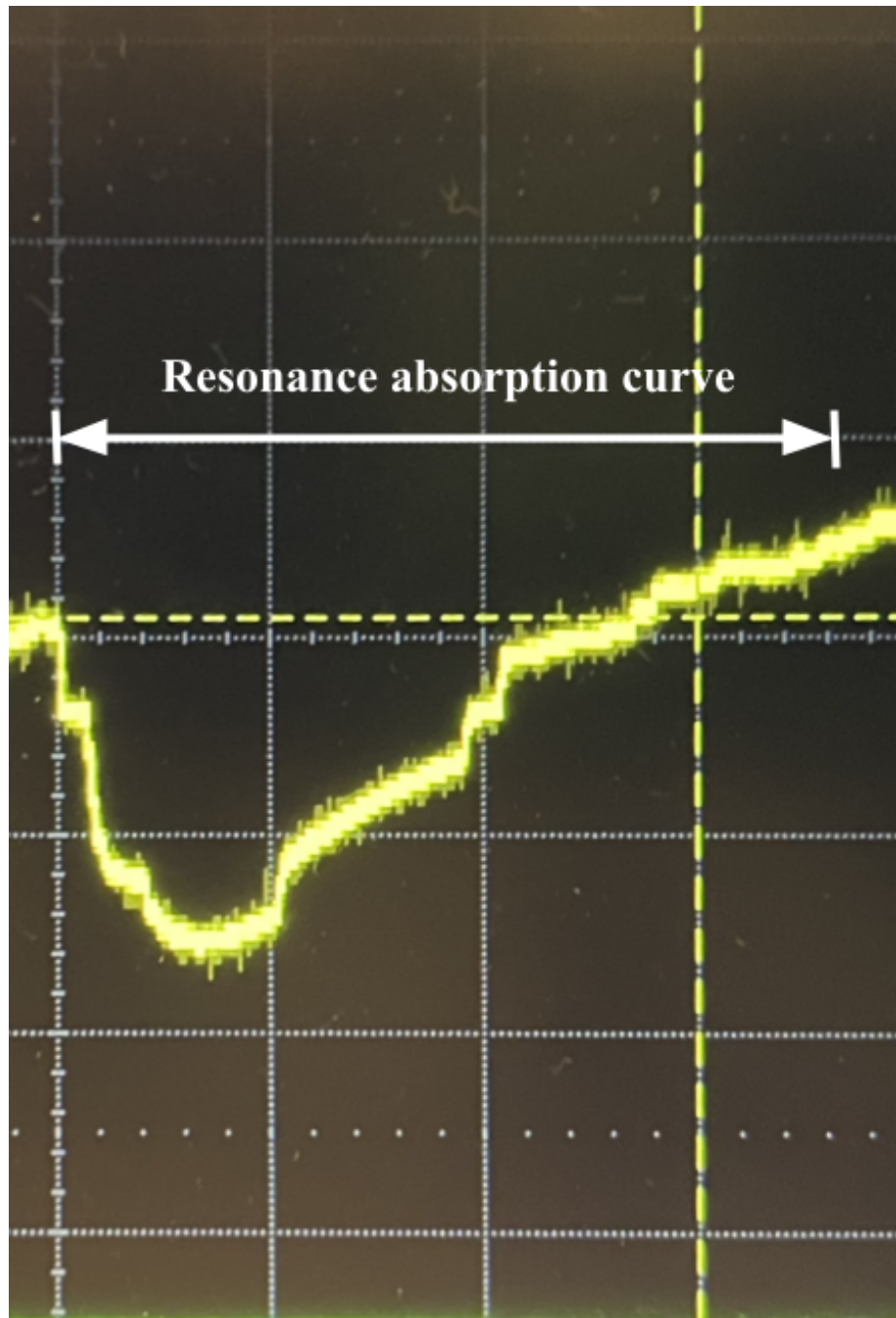


Figure 4.3: Photodiode signal for light transmitted through the rubidium vapor cell. The wavelength of the resonance was from just above the resonance at $12816.693 \text{ cm}^{-1}$ to just below the resonance. The lower the the curve, the more light that was absorbed by the rubidium in the vapor cell.

4.2 Feed-forward Scanning

For the feed-forward scanning, I used a function generator to simultaneously scan the piezo voltage and the current. The function generator allowed for a more

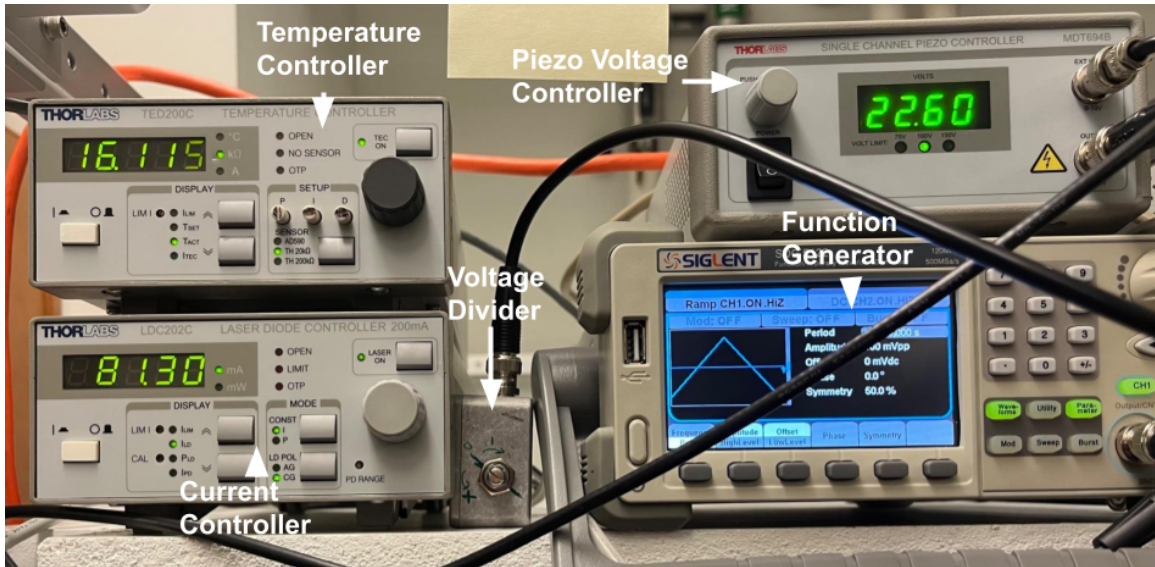


Figure 4.4: Picture of the ECDL controllers with the function generator now attached to the piezo voltage controller, and then also attached to a voltage divider which is then connected to the current controller.

precise scanning than could be done by hand for all considerations involved, such as rate of of the scanning, amount scanned, and the coordination between the piezo and the current. Thus, I attached the function generator to the current controller and the piezo controller and tested the outputs from both to ensure that it worked as expected, which it did.

In order to be able to change the scan range of the current and piezo voltage at the same time, I constructed a voltage divider using a potentiometer for the input to the current controller. Thus, I could use the function generator itself to adjust the scan range of the piezo voltage and then use the knob on the potentiometer to adjust the scan range of the current. The addition of the function generator and the voltage divider to the current controller and piezo set-up is shown in figure 4.4.

Determining Functions for Feed-Forward Scanning

Once the function generator was properly connected, my first step was to determine what kind of waveform to use. I decided on the ramp waveform for both the

piezo and the current, as this would vary the current and piezo voltage at a constant rate which in turn varies the frequency at a constant rate. The linear scan of both up and down would then allow for the cleanest image of the actual shape of the resonances achieved. The phase of the two waveforms were also put 180° out of phase so the piezo voltage increased while the current decreased and vice versa. This meant that both increased the frequency or both decreased the frequency in a feed-forward configuration.

The next step was to determine the ratio of how much the piezo should be scanned versus the current. The easiest way to determine to approximate ratio was to graph the data of when the frequency would mode hop. I started by setting the temperature and the piezo voltage to the values previously stated. I then set the current to a value high above the lasing threshold and recorded the value of the current and the piezo voltage. Then, I decreased the current until there was a mode hop and recorded the voltage and current and then increased the piezo voltage until there was a mode-hop and recorded those values. I repeated this process until there were enough values to apply a linear fit to the points on a piezo voltage versus current graph. The slope of this graph is then the approximate ratio at which the two should be scanned [6].

When I did this, the slope of fitted linear curve was approximately -0.5 mA/V as shown in figure 4.5. The negative slope is due to the 180° phase difference in the functions sent to the piezo controller and current controller respectively. The slope means that for every 1V that the piezo is changed, the current should change by half that amount (in mA). It is important to note, however, that this was only an approximate ratio.

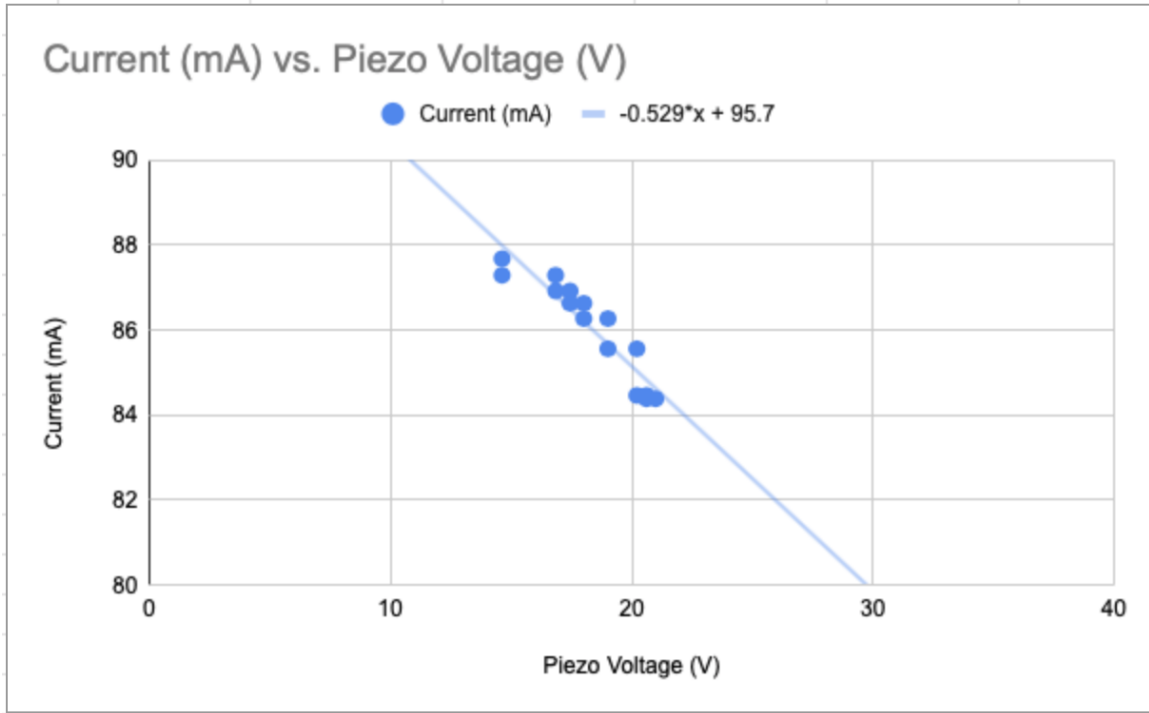


Figure 4.5: Graph of the the current (mA) versus the piezo voltage (V) of the ECDL when it mode-hopped. The dots are the actual data points, while the line is the linear fitted curve to the data, which has the equation $V = -0.5 \cdot I + 96$, where V is the piezo voltage in V in I is the current in mA.

Scanning Resonances

Once the approximate feed-forward scanning was determined, the next step was to test it and try to expand the scanning range of the ECDL. I specifically focused on increasing the scanning range near a resonance in order to see an emission curve and also because the ECDL would be used on resonance in other experiments in the lab.

I started the feed-forward scanning at the approximate ratio of -0.5 mA/V , but I also tried various other ratios in order to test the performance. Through this process, I ruled out increasing the current more than the piezo voltage, as well as having a positive ratio, as both decreased the scan range instead of increasing it. I also tried increasing the current at a even lower rate, such as -0.3 mA/V , which increased the scan range to approximately 1 GHz. I was also able to achieve about 1 GHz of scan



Figure 4.6: Picture of the oscilloscope showing the emission from the resonance detected by the photodiode due to the feed-forward scanning. The wavenumber of the laser was scanned from $12816.609 \text{ cm}^{-1}$ - $12816.649 \text{ cm}^{-1}$. The light detected by the photodiode is shown in yellow, where shown in the red box, two slightly separated resonances are visible. The feed-forward scan of the current is shown in pink and the feed-forward scan of the piezo is shown in blue. The piezo voltage was scanned over 2V while the current was scanned over 1mA.

range with other ratio close to -0.5 mA/ V , such as -0.4 mA/ V and -0.75 mA/ V . However, the highest scan range I was able to achieve was with a ratio of -0.5 mA/ V , which was 1.3 GHz. I was able to get this scan range at about 12816.62 cm^{-1} , shown in figure 4.6, and at 12816.5 cm^{-1} . To get this scan range, I used the ramp function as stated previously to scan both the current and piezo voltage, and I scanned the piezo voltage over 2.6 V centered at 23.08 V, and the current over 1.3 mA centered at 85.44 mA.

In figure 4.6, it is possible to see that the resonance at about 12816.62 cm^{-1} actually consists of two separate resonances. This is known as one would expect a singular resonance to go up to its maximum value and then decrease and then this

would repeat as the piezo voltage and current scanned back and forth. However, in the scan obtained, the emission from the vapor cell increases, then decreases slightly in the middle of the scan, increases slightly, and then decreases. This pattern is then repeated once the piezo voltage and current scanning reverse directions. These resonances are close enough that to the eye it appears to be one resonance due to the broadened resonances, but due to the scanning range of the ECDL and the measurement from the photodiode, it is possible to see the splitting of the resonances.

4.3 Measuring Linewidth

Once feed-forward scanning was optimized as best possible in the time available, I moved onto measuring the linewidth of a new laser obtained by the lab, a 780 nm Distributed Bragg Reflector (DBR) laser with a butterfly housing, as shown in figure 4.7. The linewidth of the ECDL was previously measured to be, at maximum, 0.5 MHz [2]. Since the linewidth of the ECDL is significantly smaller than the expected linewidth of the DBR laser, the light from the ECDL and the DBR laser could be combined to measure the linewidth of the DBR laser using the FWHM of the beat note, as described in equation 2.3.

To measure the beat note, I attached both lasers to a fiber optic combiner and then measured the output using a photodetector attached to a spectrum analyzer, as shown in figure 4.8. I had to ensure that both lasers were at similar frequencies, as the spectrum analyzer and fast photodiode have limited frequency ranges so a large difference in frequencies meant the resultant beat note would not be able to be measured. However, the frequencies could not be the same as then there would be no beat note. I also used a resonance frequency so that I could easily tell if the ECDL mode-hopped in the midst of taking data by looking at rubidium vapor cell on the CCTV. I therefore set both lasers to approximately 12816.5 cm^{-1} and then adjusted

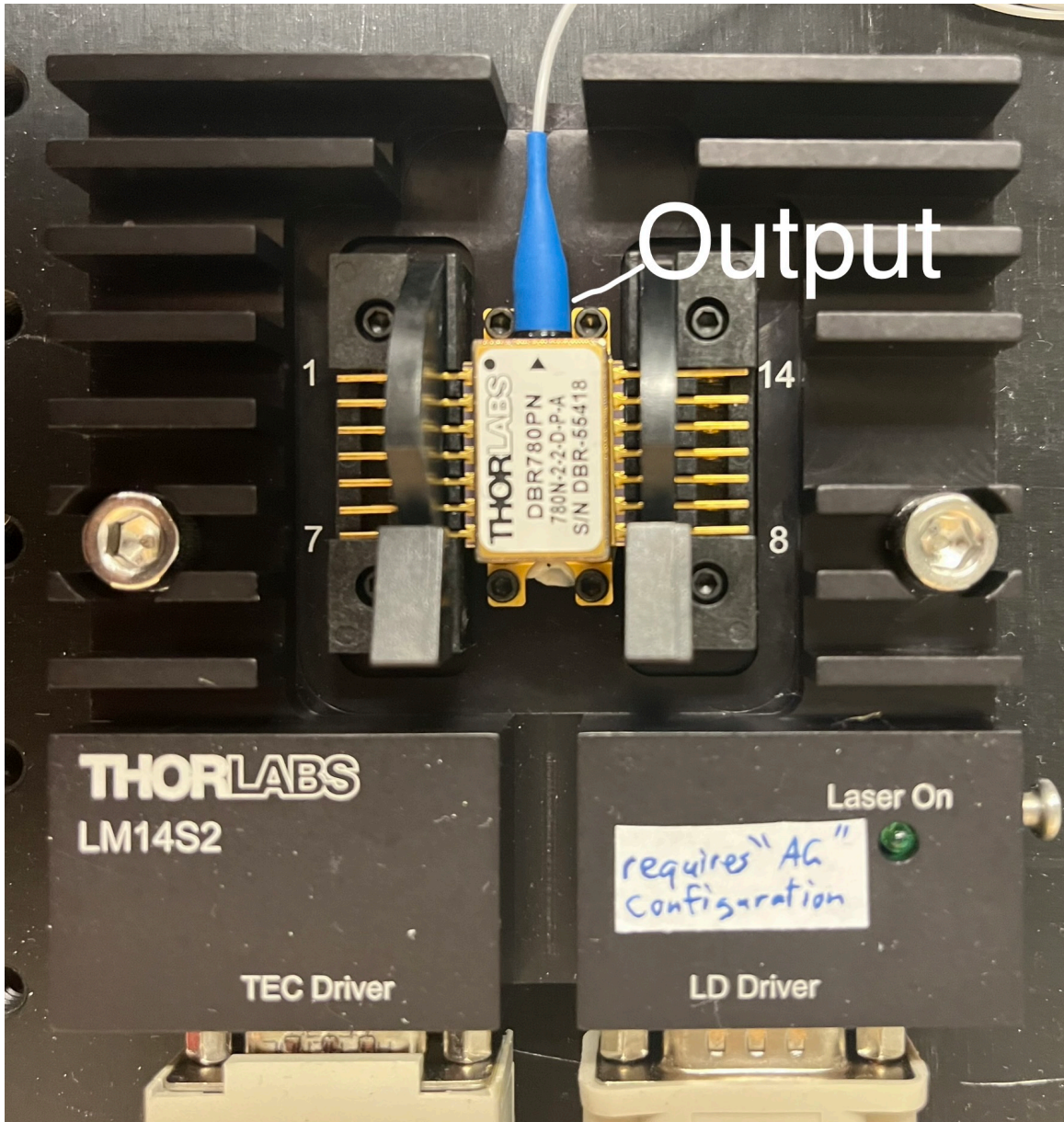


Figure 4.7: Picture of the DBR laser from the lab of which the linewidth was measured.

the DBR laser until I could see the beat note on the spectrum analyzer.

Using the spectrum analyzer, I slowly zoomed in on the beat note in order to get a more precise measurement of it. The closest I achieved was a horizontal scan range of 100 MHz, divided by 10 boxes so each box was 10 MHz, and then a vertical range of 2 mV, again divided by 10 boxes so each box was 0.2 mV tall. However,

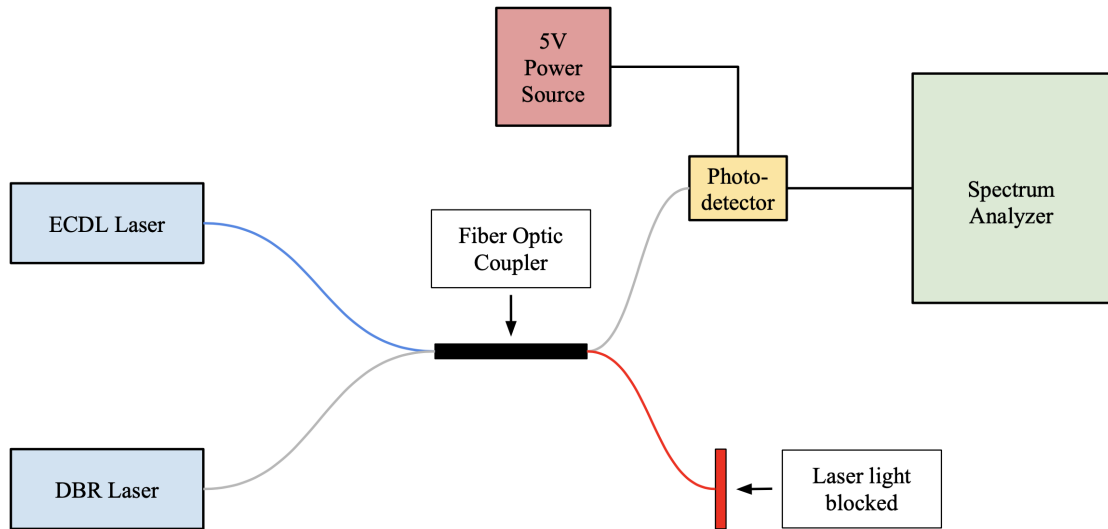


Figure 4.8: Diagram of the set-up used to measure the linewidth of the DBR laser using the ECDL. The DBR laser and the ECDL are both connected and input into the coupler. From there, half of the combined output goes to the red fiber and is then blocked and half the combined output goes through the light gray fiber. From there, the light is sent to a photodetector which is powered by a 5V power source. The output from the photodetector is then sent to a spectrum analyzer.

since the spectrum analyzer operates such that it scans the range, measuring each box consecutively and not simultaneously, different measurements led to different linewidth measurements. This is likely due to the movement of the beat note as the frequencies of the input lasers slightly shifted throughout the measurements. This shift became more obvious as I zoomed in on the beat note as it was easier to see the slight shifts in the frequencies and thus in the shape of the beat note.

As shown in figures 4.9 and 4.10, the height of the beat note is 0.6 mV, or 3 boxes, so the half-maximum is 0.3 mV, or 1.5 boxes. However, the FWHM for the beat note measured was as large as 8 MHz as seen in figure 4.9 or as small as 3 MHz as seen in figure 4.10. The larger linewidth is likely due to the laser frequency moving with the sweep of the spectrum analyzer, broadening the beatnote, while the smaller linewidth is likely due to the laser frequency moving opposite the sweep of the spectrum analyzer, narrowing the beatnote. While the smaller linewidth would

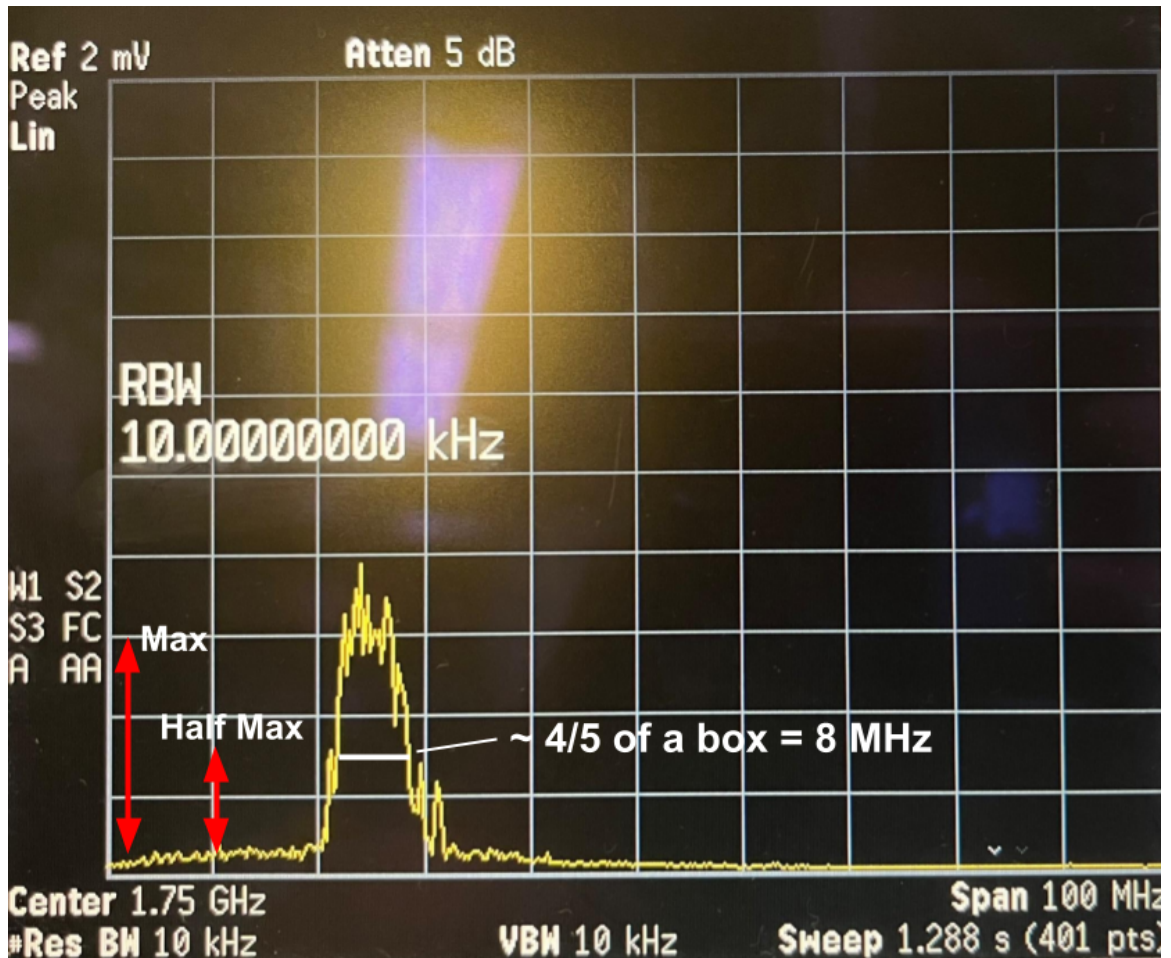


Figure 4.9: The linewidth measurement of the beatnote between the ECDL and the DBR laser using the spectrum analyzer. The yellow line is the signal from the photodetector. Each box for box is 10 MHz wide and 0.2 mV tall. The FWHM of the beatnote is 8 MHz.

be preferred, I was unable to get a more precise value using the ECDL.

In order to get a better measurement of the linewidth, I used a different laser in the laboratory that was more stable and had a quoted linewidth of 100 kHz, which is even smaller than the ECDL [15]. This laser resulted in a more stable beatnote, so I was able to get a more precise value of the linewidth as the shape of the peak varied less with this laser than with the ECDL. Thus, I measured the linewidth of the DBR laser to be 5 MHz, as shown in figure 4.11. This is close to the average found using the ECDL, showing that the ECDL, while not as precise as the other laser, still worked in measuring approximately the same linewidth.

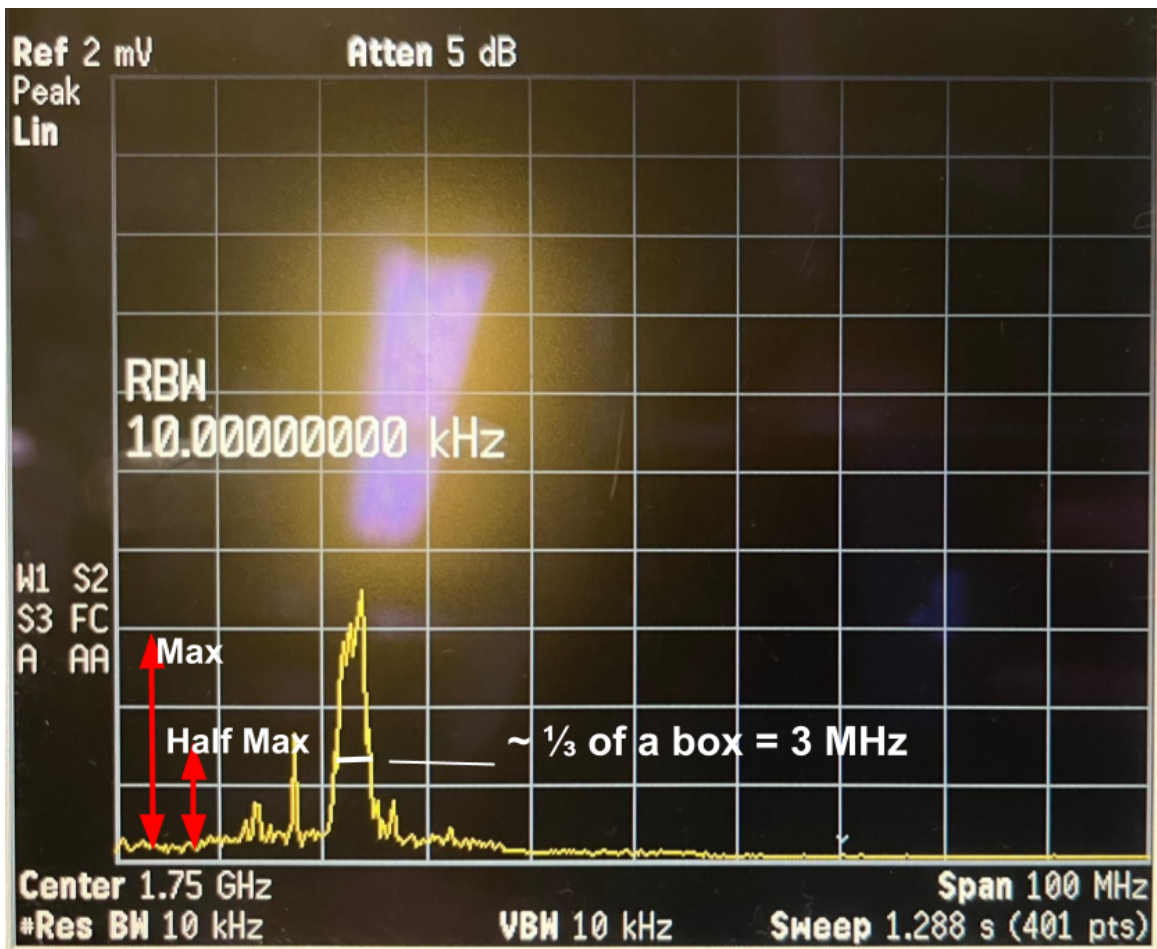


Figure 4.10: The linewidth measurement of the beatnote between the ECDL and the DBR laser using the spectrum analyzer. The yellow line is the signal from the photodetector. Each box for box is 10 MHz wide and 0.2 mV tall. The FWHM of the beatnote is 3 MHz.

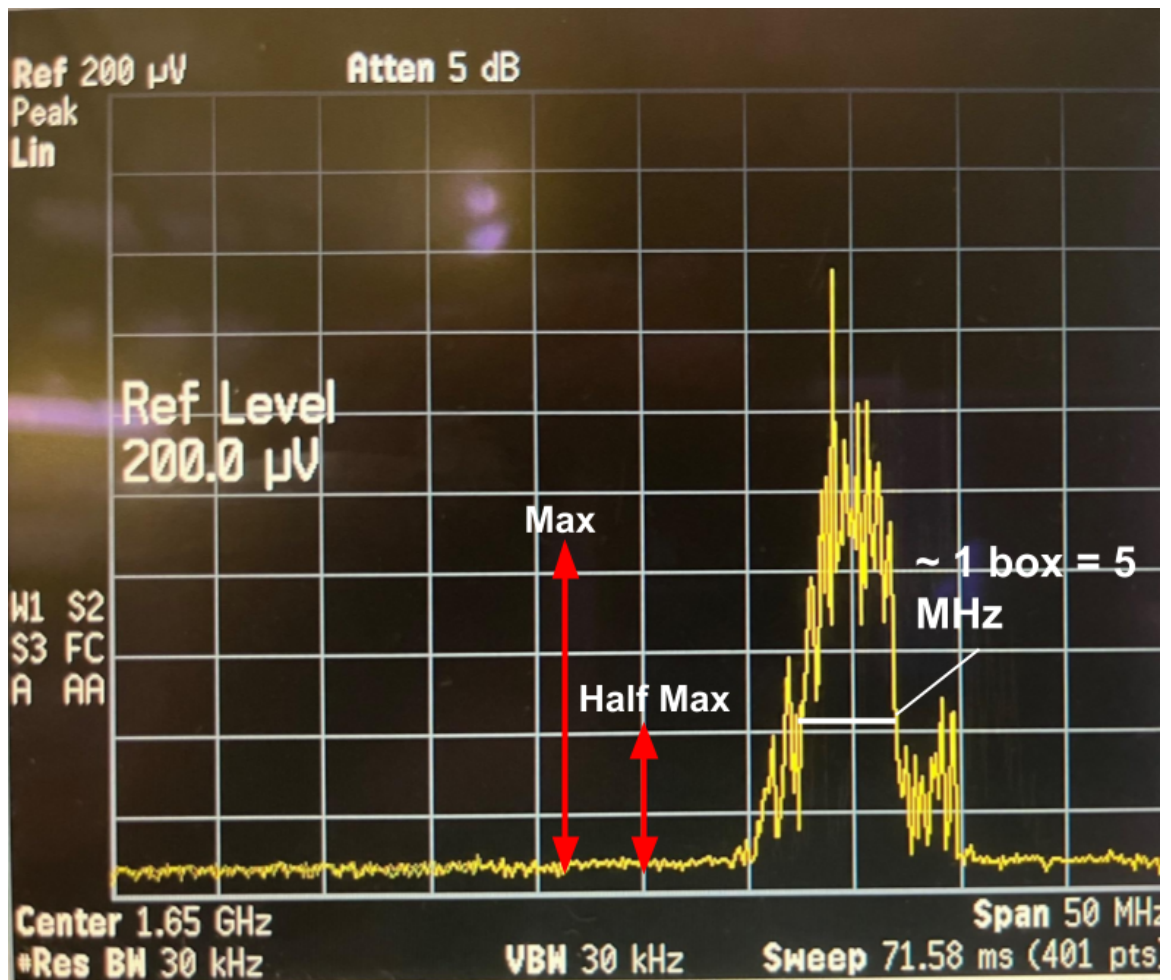


Figure 4.11: The linewidth measurement of the beatnote between the laser with a 100 kHz linewidth and the DBR laser using the spectrum analyzer. The yellow line is the signal from the photodetector. Each box for box is 5 MHz wide and 20 μV tall. The FWHM of the beatnote is 5 MHz.

Chapter 5

Conclusion

5.1 Summary of Results

This project demonstrated tangible improvements to the existing ECDL. This included obtaining a feed-forward scan range of 1.3 GHz. While this is significantly less than the desired scan range of 10 GHz needed to scan the full range of the rubidium D2 transitions, it was an improvement from scanning without feed-forward. In addition, this scanning was much more stable than previous attempts by other experimenters, as the laser was able to remain on resonance on the scale of minutes as opposed to tens of seconds. This may be due to the added stability from the additional thermal housing as the laser's frequency is sensitive to changes in temperature.

The second part of this project showed an application of the ECDL in measuring the unknown linewidth of another, new laser in the laboratory. This was useful information in order to inform future experiments with the other laser. The linewidth of the laser was determined to be 5 ± 3 MHz. The large uncertainty in the laser's linewidth is due the changing shape and size of the beat note due to its shift in frequency as both the ECDL and the DBR laser drifted in frequency. Thus, the beat note may have shifted as the spectrum analyzer scanned the frequencies resulting in the beat note appearing more broad if it shifted to a higher frequency or less broad if

it shifted to a lower frequency than it actually was. When the linewidth was measured using a different laser, however, the linewidth was found to be 5 MHz, which is the same as was found when using the ECDL but with less uncertainty. The precision of the linewidth measurement from the ECDL could be improved by waiting longer before taking measurements after turning on the laser to allow the temperature to stabilize. This would stabilize the frequency and thus stop the beatnote from moving around, distorting its shape. It would also allow the scan range of the spectrum analyzer to be decreased, increasing the precision of the FWHM measurement.

5.2 Outlook

Overall, the main contribution of this thesis was getting the ECDL operating and reconfigured after years of little to no use. I assembled and aligned an optics set-up for the laser from scratch, determined the lasing threshold of the laser, and figured out what parameters were necessary to achieve rubidium resonances. It was a long process of learning how to determine when the ECDL was getting close to a resonance and when it was about to mode-hop. Now, I understand how the ECDL works and can obtain a resonance in a matter of minutes as opposed to the days or hours it took me at the beginning of this project.

There are a few short-term steps that could be completed with the ECDL as it currently operates. The first step would be to get a more precise linewidth measurement by taking more measurements and minimizing the scan range on the spectrum analyzer. These steps were not taken for this thesis due to time constraints, and the fact that the photodiode that was initially used broke.

Another more short-term experiment would be to do saturation spectroscopy by scanning the ECDL frequency over a resonance for as long as possible. From this, one would be able to get a clearer measurement of the hyperfine splittings of the

resonance. This would also demonstrate the stability and range of the ECDL and thus its usefulness.

The long-term improvement necessary for the ECDL to have wider use in the laboratory is to increase its scan range. With an increased scan range the ECDL would be able to easily achieve all the rubidium D2 resonances, allowing the ECDL to be used in the process of laser cooling of rubidium. Now that less time is needed to achieve a resonance, more time could be spent on optimizing the feed-forward capabilities at the resonance frequencies. Once the feed-forward scan range is increased to at least a few GHz, if not 10 GHz as was the original goal (though that may not be possible), the laser could then be tuned to 776 nm. At this new wavelength and through optimizing the feed-forward scanning at this wavelength, various new measurements could be made, such as testing the 2-photon transition of rubidium in a vapor cell, measuring the 5D hyperfine splittings, and investigating the electromagnetically induced transparency of probe lasers for locking the ECDL on a specific 5D transition. Then, the 2-photon transition of to the 5D states of rubidium could be tested in the magneto-optical trap, as well as measuring the hyperfine splittings. The longest-term objective relating to this project would then be to develop a 1258 nm ECDL in order to eventually reach a Rydberg Stark manifold.

Bibliography

- [1] B. Halkowski, “External Cavity Diode Laser for Ultra-cold Atom Experiments”, Honors Thesis (College of William and Mary) (2018).
- [2] Q. Olson, “Thermal, Mechanical, and Electrical Engineering of an External Cavity Diode Laser”, Senior Thesis (College of William and Mary) (2019).
- [3] M. Kienlen, N. Holte, H. Dassonville, A. Dawes, K. Iversen, R. McLaughlin, and S. Mayer, “Collimated blue light generation in rubidium vapor,” *American Journal of Physics*, 81, 442-449 (2013).
- [4] R. Pooser, A. Marino, V. Boyer, K. Jones, and P. Lett, “Quantum correlated light beams from nondegenerate four-wave mixing in an atomic vapor: The D1 and D2 lines of 85Rb and 87Rb,” *Optics Express*, 17, 16722-30 (2009).
- [5] E. K. Dietsche, A. Larrouy, S. Haroche, J. M. Raimond, M. Brune, and S. Gleyzes, ”High-sensitivity magnetometry with a single atom in a superposition of two circular Rydberg states,” *Nature Physics*, 15, 326 (2019).
- [6] S. Charles Doret, ”Simple, low-noise piezo driver with feed-forward for broad tuning of external cavity diode lasers”, *Rev. Sci. Instrum.*, 89 (2018).
- [7] J. Beyer and S. Wilkinson, ”Tuning thermal PID loops”, *Control Engineering*.
- [8] M. Harris, R. Loudon, T.J. Shepherd, and J.M. Vaughan, ”Mode-hopping hysteresis in a single-frequency laser”, *Optics Communications*, 101, 432-441 (1993).

- [9] S. Huang, T. Zhu, M. Liu M, and W. Huang, "Precise measurement of ultra-narrow laser linewidths using the strong coherent envelope", *Sci Rep.*, 7, 41988 (2017).
- [10] R. Paschotta, "External Cavity Diode Lasers", *RP-Photonics Encyclopedia*, (2023).
- [11] D. Griffiths, "Introduction to Electrodynamics", (2013).
- [12] H. Ball, M. Lee, S. Gensemer, and M. Biercuk, "A high-power 626 nm diode laser system for Beryllium ion trapping," *The Review of scientific instruments*, 84, 063107 (2013).
- [13] C.E. Png, S. Chan, S. Lim, and G. Reed, "Optical Phase Modulators for MHz and GHz Modulation in Silicon-On-Insulator," *Journal of Lightwave Technology*, 22, 1573- 1582 (2004).
- [14] D. Preston, "Doppler-free saturated absorption: Laser spectroscopy", *American Journal of Physics*, 64, 1432 (1996).
- [15] "DL Pro", Toptica.